



Study of cerebrovascular reactivity to hypercapnia by imaging photoplethysmography to develop a method for intraoperative assessment of the brain functional reserve

MAXIM A. VOLYNSKY,^{1,2,6}  OLEG V. MAMONTOV,^{2,3,6} ANASTASIIA V. OSIPCHUK,⁴ VALERY V. ZAYTSEV,^{2,3} ALEXEY Y. SOKOLOV,^{4,5} AND ALEXEI A. KAMSHILIN^{2,3,*} 

¹*School of Physics and Engineering, ITMO University, 49 Kronverksky av., 197101 St. Petersburg, Russia*

²*Laboratory of New Functional Materials for Photonics, Institute of Automation & Control Processes of the Far East Branch of the Russian Academy of Sciences, 5, Radio str., 690041 Vladivostok, Russia*

³*Department of Circulation Physiology, Almazov National Medical Research Centre, 2 Akkuratov str., 197341 St. Petersburg, Russia*

⁴*Department of Neuropharmacology, Valdman Institute of Pharmacology, Pavlov First Saint Petersburg State Medical University, 6-8 Lev Tolstoy str., 197022 St. Petersburg, Russia*

⁵*Laboratory of Cortico-Visceral Physiology, Pavlov Institute of Physiology of the Russian Academy of Sciences, 6 Makarov emb., 199034 St. Petersburg, Russia*

⁶*These authors contributed equally to this work*

**alexei.kamshilin@yandex.ru*

Abstract: Intraoperative assessment of cerebrovascular reactivity is a relevant problem of neurosurgery. To assess the functional reserve of cerebral blood flow, we suggest using imaging photoplethysmography for measuring changes in cortical perfusion caused by CO₂ inhalation. Feasibility of the technique was demonstrated in three groups of anesthetized rats ($n=21$) with opened and closed cranial windows. Our study for the first time revealed that the hemodynamic response to hypercapnia strongly depends on the cranial state. However, it was shown that regardless of the direction of changes in local and systemic hemodynamics, the ratio of normalized changes in arterial blood pressure and cortical perfusion could be used as a measure of the cerebrovascular functional reserve.

© 2021 Optical Society of America under the terms of the [OSA Open Access Publishing Agreement](#)

1. Introduction

Assessment of the functional reserve of cerebral blood flow in the conditions of surgical intervention on the vessels of the brain is a relevant problem of neurosurgery. The solution to this problem is necessary both to clarify the degree of hemodynamic significance of intracranial artery stenosis and to control the effectiveness of the surgical treatment. To date, two methods, Positron Emission Tomography and Magnetic Resonance Imaging, are most frequently used for assessment of this parameter by applying functional tests with vasodilators [1,2]. The most commonly used vasodilator is a carbonic anhydrase inhibitor, acetazolamide, whose vascular effect is realized both directly and due to the development of metabolic acidosis [3,4]. However, it is known that CO₂ is a substance most actively promoting the dilatation of cerebral vessels [5].

The dilatation of cerebral arteries in hypercapnia is associated with various mechanisms, in particular, a CO₂-mediated decrease in pH, an increase in the release of potassium from the smooth muscle cells of the vascular wall, as well as an increase in the expression of NO synthase with the accumulation of nitric oxide [6,7]. In addition, the hypercapnia triggers reflexes through peripheral and central chemoreceptors: their activation increases cerebral blood flow by raising systemic blood pressure in response to augmented activity of the sympathetic nervous system. At

the same time, against the background of sympathicotonia, bradycardia may develop, the origin of which is associated with compensatory activation of the parasympathetic nervous system [8,9]. Sympathetic-mediated increase in vascular tone prevents a decrease in blood pressure in response to the direct dilatation effect of CO₂ on peripheral vessels, although it is often excessive. However, despite the increase in the tone of the peripheral arteries, cerebral vessels easily avoid systemic exposure due to cerebrovascular autoregulation [10].

Therefore, any change in cerebral blood flow in response to CO₂ alteration can be used to assess cerebral vasomotor reactivity [2,11–13]. Note that both hypercapnic (inhalation of carbon dioxide, voluntary breath holding, breathing in a closed circuit, etc.) and hypocapnic (hyperventilation) functional tests are used. Besides Magnetic Resonance Imaging and Positron Emission Tomography, vascular responses can be assessed using Transcranial Doppler Ultrasound [14], Dynamic Computed Tomographic Imaging [15], Single-Photon Emission Computed Tomography [16,17], Time-Resolved NIR Spectroscopy [18,19], and Laser Doppler Flowmetry [20–22], both during clinical practice and with experimental animals. Nevertheless, in most cases, the assessment of cerebral blood flow is carried out with an intact skull, a rare exception is the use of Laser Doppler Flowmetry [23,24] or Magnetic Resonance Imaging [25,26] during neurosurgery or after traumatic brain injury, although such applications are rather limited and not very informative. However, most neurosurgical operations are performed with craniotomy, but the very complex nature of the effect of the vasodilator on cerebral hemodynamics suggests that it may differ significantly from the case of an intact skull. At the same time, it is very important for the surgeon to receive an objective assessment of the functional reserve directly during the surgery and as quickly as possible.

Recently, in experiments on rats, we demonstrated that an imaging photoplethysmography (iPPG) is an easy-to-use, contactless method for assessing the functional reserve of the cortical vascular network during the test with a carbonic anhydrase inhibitor [27]. It was shown that the heart-related pulsations amplitude in cerebral tissues quantified by the parameter amplitude of pulsatile component (APC) is a marker of the vascular tone [10,27].

The objectives of this study are (i) to verify feasibility of using iPPG as a technique for monitoring cerebrovascular reactivity during neurosurgical interventions, (ii) to compare the effects of CO₂ inhalation-induced hypercapnia on systemic hemodynamics and intracranial blood flow in rats with intact and trepanned skulls, and (iii) to assess the effect of the hypercapnia duration on the change in the parameters of cortical blood flow. All set objectives have been successfully achieved.

2. Materials and methods

2.1. Animals and ethics

The experiments were performed in accordance with the ethical guidelines of the International Association for the Study of Pain, the Directive 2010/63/EU of the European Parliament and of the Council on the protection of animals used for scientific purposes and reported in compliance with the ARRIVE guidelines. The study protocol was approved by the Institutional Animal Care and Use Committee of Pavlov First St. Petersburg State Medical University (decision No. 03/20-DN) before carrying out the experiments. Every effort has been made to minimize animal suffering, and as many animals as necessary were used in experiments to obtain reliable data.

Adult (mean body weight 407 ± 106 g, $n = 21$) male Wistar rats were purchased from the State Breeding Farm “Rappolovo” (Saint Petersburg, Russia). The animals were housed in groups (2–5 per cage) under standard laboratory conditions (12-h light/dark schedule) with food and water available ad libitum.

2.2. Anesthesia and surgical preparation

Rats were anaesthetized by intraperitoneal injection with a mixture of urethane (Sigma, St. Louis, MO, USA) and α -chloralose (Sigma, St. Louis, MO, USA) at an initial dose of 800/60 mg/kg. Once a surgical level of anesthesia was achieved, the trachea was intubated for artificial pulmonary ventilation and assessment of end-tidal carbon dioxide, the right femoral artery and vein were cannulated for continuous monitoring of blood pressure and drug administration, respectively. The animal's head was fixed in a stereotaxic apparatus (Stoelting Co., Wood Dale, IL, USA) for preparation of a cranial window. Contactless assessment of cerebral blood flow in 8 rats was carried out by the iPPG system in conditions of closed skull. To achieve this, the parietal bone was thinned using a micro-drill until the intracranial vessels were clearly visible through the remaining intact bone. During the drilling, tissues were cooled using topical application of cold saline. The surface of the closed cranial window was covered with mineral oil to improve the transparency of the residual bone for intravital video recordings of intracranial vessels. In another 13 rats, cerebral blood flow was assessed in the open cranial window after removal of a part of the parietal bone. There were two cranial windows for the right and left hemispheres measuring approximately 7.0 - 7.5 mm by 3.8 - 4.2 mm that occupied about 20% of the skull area. For these rats, two series of measurements were performed. We first measured the hemodynamic parameters of these 13 animals under intact dura mater conditions, and then all measurements were repeated after removal of the dura mater. Therefore, two groups of the experimental data (with and without dura mater) were obtained on the same rats that allows us to minimize the number of laboratory animals used.

Steel needle electrodes were installed in the muscle tissue of rat paws to record the electrocardiogram (ECG) during the experiment. After surgical preparation, the rat rested for at least 40 min to minimize the effect of postsurgical reaction. All animals were paralyzed with pipecuronium bromide (0.9 mg/kg initially; maintained with 0.45 mg/kg as required, i.v.; "Arduan", Gedeon Richter, Budapest, Hungary) and artificially ventilated with room air (SAR-830, CWE, Inc., Ardmore PA, USA). Artificial ventilation was carried out at a frequency of 50 breaths per minute, and the gas flow was regulated individually both for each animal and during the experiment, depending on the general physiological parameters.

Throughout all experiments, the rectal temperature was monitored and maintained within a range of 37–38 °C using a thermostatically controlled heating pad. Arterial blood pressure (ABP) and end-tidal CO₂ were continuously monitored by a pressure transducer (MLT844, AD Instruments Inc., Colorado Springs, USA) and Carbon Dioxide Analyzer (Capstar-100, CWE, Inc., Ardmore PA, USA), respectively. These data were digitized at the sample frequency of 10 kHz (ADC-DAC Power1401-3, Cambridge Electronic Design, Cambridge, UK) and recorded in the personal computer using Spike2 version 8 software (Cambridge Electronic Design, Cambridge, UK). The adequacy of anesthesia was controlled by absence of withdrawal reflex after paw pinch (before myorelaxation) or severe (> 20%) blood pressure fluctuations (after myorelaxation). If necessary, a supplemental dose of the anesthetic mixture of urethane/ α - chloralose (75/5 mg/kg) was administered intravenously.

2.3. Experimental protocol

The total duration of each experiment was 600 s during which video frames of intracranial structures were recorded continuously and synchronously with ECG, ABP, and end-tidal CO₂ content. Based on these measurements, the heart rate (HR) was calculated as the inverse time between R-peaks in the ECG signal, and the pulse pressure (PP) was calculated from the ABP data. Parameter APC of the PPG waveform was calculated from the sequence of video frames using R-peaks of the ECG signal as a cardiac timing Ref. [28].

First, all these parameters of the rat in the baseline were recorded during the first 60 s of each experimental session.

Second, artificial ventilation with room air was replaced by ventilation with a mixture of air and CO₂ in the ratio of 95% and 5%, respectively. In each case when the ventilation mode was changed, the inhaled volume and respiratory rate remained unchanged. For rats with closed skull, three experimental sessions were carried out with different times of inhalation of CO₂ mixture in ascending order: for 30, 60, and 120 s. We have designated this group of experimental sessions as closed cranial window (CCW). For rats with open skull, similar three experimental sessions with dura mater were first carried out. This was followed by the same three sessions were carried out after removal of the dura mater. The experimental sessions with rats having open skull but intact dura mater were designated as OSD, whereas sessions with open cranial window and dura mater removed called as OCW. The time for switching from one mode of artificial ventilation to another was no more than 10 s.

Third, artificial ventilation was returned to the mode with room air, and all the aforementioned parameters were continuously recorded until the end of the 10th minute starting from the beginning of each session.

2.4. *Experimental arrangement*

To evaluate the parameters of blood flow and other physiological parameters of the animal, we used the same experimental setup in our previous work [27]. The difference in the configuration of these setups is as follows. While in the previous study [27] the injection of dorzolamide was used as the cause of the change in hemodynamic parameters, in the present work the functional effect was achieved by inhalation of an air mixture with an increased content of CO₂. Technically, the breathing mode was changed by switching the breathing mixture selection valve from room air to a cylinder with a prepared mixture and vice versa. The key-component of both setups is a custom-made iPPG system. Briefly, the system consisted of a digital monochrome camera with complementary metal-oxide-semiconductor sensing matrix (10-bit model GigE uEye UI-5220SE of the Imaging Development Systems GmbH, Germany) and illumination block. The latter contained eight light-emitting diodes (LEDs) mounted around the camera lens (Computar M1214-MP2, Japan, 25 mm focal length) in such a way as to ensure uniform illumination of the rat's cortex through the cranial window. Incoherent light generated by LEDs at the wavelength of 530 ± 25 nm was linearly polarized by means of a film polarizer (Edmunds Optics, USA, 0.18 mm thickness) attached to the LED assembling. To increase the signal-to-noise ratio, we used the polarization-filtration technique implemented in the form of another film polarizer (with orthogonal orientation to the first one) attached to the camera lens [29]. The iPPG system with LEDs and polarizers was located 15 cm above the rat's cortex. The videos were recorded at 100 frames per second with resolution of 752×480 pixels and saved frame-by-frame in the solid-state hard disk of a personal computer.

2.5. *Data processing*

All recorded video frames, ECG, ABP and CO₂ were analyzed off-line using custom software implemented in the MATLAB platform (Version R2020a, The MathWorks, Inc., MA, USA, 2020). The analysis was performed over the entire surface of the cranial window, excluding areas with highlights and artifacts (e.g., hematomas). At each moment in time, the PPG waveform was assessed in every small region of interest (ROI) of size 11×11 pixels that correspond to an area of 0.24×0.24 mm² at the rat's cortex by the algorithm described in detail in our previous articles [10,27,30]. In brief, the algorithm starts with stabilizing the digital image using sectorial optical flow algorithm [28], then PPG waveform is computed as frame-by-frame evolution of the mean pixel value in every ROI and normalized by calculating the ratio of the alternating component (AC) and slowly varying (DC) component (AC/DC ratio). The time limits for each heartbeat were determined using the R-peaks of a synchronously recorded ECG. Thereafter, a mean PPG pulse was calculated by averaging the waveforms of 12 subsequent heartbeats. Finally,

the parameter APC was calculated as difference between the maximum and minimum values of the mean PPG pulse. Physiologically, it indicates changes in arterial blood volume due to their pulsating nature: the greater variations of the vessels diameter regulated by the arterial tone, the higher amplitude of pulsations, i.e. APC [10].

The parameter APC was first calculated in every ROI and then averaged over the selected area. Note that the analysis of data collected over the entire cranial window followed by averaging does not lead to information loss but increases its reliability because it was shown that PPG waveforms from large vessels are rather similar to waveforms from sites between vessels [27]. Parameter ABP was recorded in the computer at the sample rate of 10 kHz. Based on these data, PP was calculated as the peak-to-foot ABP in each cardiac cycle, corresponding to the difference between systolic and diastolic pressure. HR was also calculated for each cardiac cycle using ECG data as the reciprocal time between adjacent R-peaks.

2.6. Statistical analysis

In the statistical analysis of the data, not all experimental sessions were used, since some of them were considered irrelevant by expert judgment (for example, due to the unsatisfactory general physiological state of the animal by the end of the experimental session). The number of experimental sessions in each group of rats are presented in the Table 1. Comparison of changes in all analyzed physiological parameters was performed using the Wilcoxon sign-rank test due to small sample sizes and deviations from the normal distribution within the samples as checked by the Komlogorov-Smirnov test. To calculate the correlation between various physiological parameters, the Pearson correlation coefficient was used. The level of significance in all statistical indicators is at least $P < 0.05$, unless otherwise indicated below. All statistical analysis was performed using the Statistica 10 software (StatSoft, Russia).

Table 1. Sample sizes by groups of experimental sessions

Hypercapnia duration	CCW	OSD	OCW
30 s	$n = 7$	$n = 13$	$n = 9$
60 s	$n = 8$	$n = 13$	$n = 10$
120 s	$n = 8$	$n = 11$	$n = 9$

3. Results

3.1. Difference in hemodynamics response on CO_2 in rats with open and closed skulls

Our study has revealed that the reaction of both systemic and cerebral hemodynamics on hypercapnia strongly depends on the conditions in which the cerebral vessels are surrounded. Three groups of experimental sessions were carried out: CCW, OSD, and OCW. The median ABP [lower - upper quartiles] during baseline was 55 [49–69], 66 [57–74], and 68 [45–70] mmHg for animals from the CCW, OSD, and OCW groups, respectively. Initial median CO_2 concentration was 1.81 [1.57-1.88] %, 1.55 [1.44-1.69] %, and 1.72 [1.60-1.76] % for the CCW, OSD, and OCW groups, respectively. There were no statistically significant differences between the initial physiological parameters of ABP and CO_2 of animals in different groups, $P > 0.05$, Wilcoxon rank-sum test.

Figure 1 shows the dynamics of changes in various measured parameters (averaged separately for each group of rats) in response to hypercapnia for 30 s. Comparing columns A and C in Fig. 1, one can see multidirectional changes in hemodynamic parameters: if in the CCW group both blood pressure (ABP, systemic parameter) and the amplitude of blood pulsations (APC, local cerebral parameter) increased, then in the OCW group both of these parameters decreased.

Notably that in the OSD group (column B), a decrease in systemic ABP did not lead to a decrease in the local cerebral APC parameter, in contrast to the OCW group.

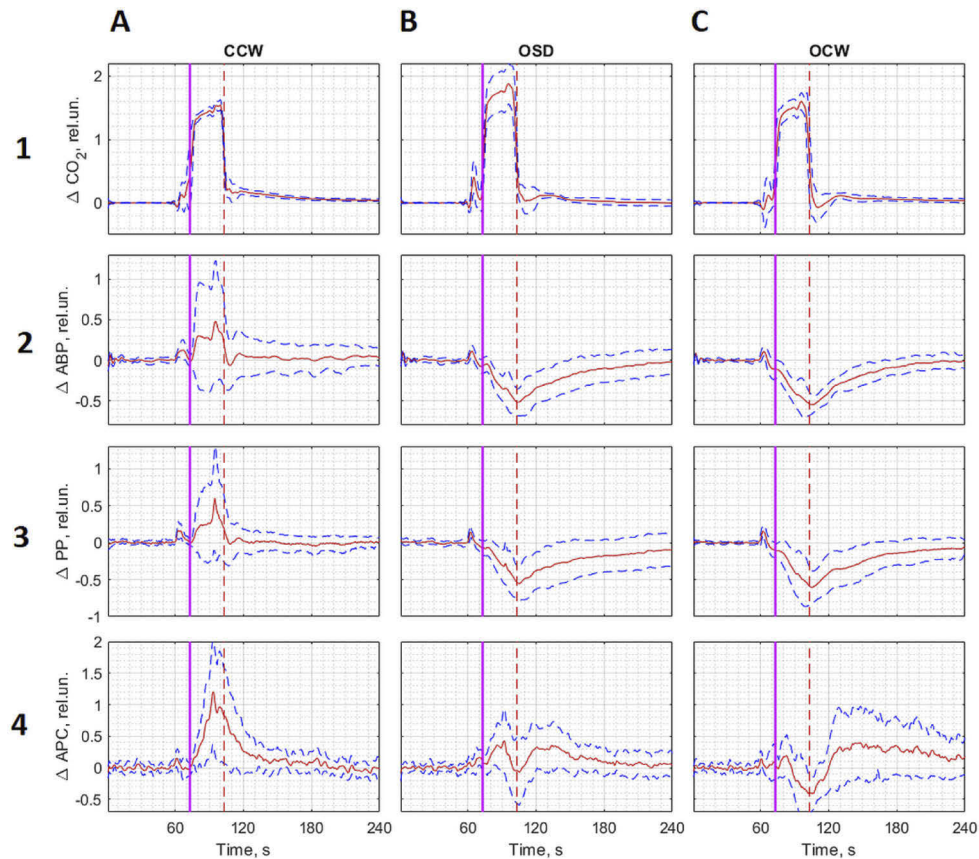


Fig. 1. Reaction of systemic and local hemodynamics in rats with different skull states to hypercapnia of 30-s duration. Columns (A), (B), and (C) shows the graphs for the groups of rats with closed cranial window, open skull but intact dura, and open skull with removed dura, respectively. Row (1) shows relative changes (in respect to the baseline) in the concentration of end-tidal carbon dioxide (ΔCO_2) averaged over each group of rats. Row (2) is the mean relative dynamics of the systemic arterial blood pressure (ΔABP). Row (3) is the mean relative dynamics of the pulse pressure (ΔPP). Row (4) shows relative changes in the amplitude of the pulsatile component (ΔAPC) also averaged over each group of animals. Initial data for estimating ΔABP and ΔPP were measured invasively through a cannula in the animal's femoral artery. The red solid lines in the graphs are the mean values of each parameter, whereas dashed blue lines show the mean \pm standard deviation. Vertical bold magenta and dashed red lines indicate the beginning and end of hypercapnia, respectively. Axis labels and scale grids are identical for every column and every row.

Note that in most cases, the recovery of parameters begins immediately after the end of hypercapnia, regardless of its duration. It is also noteworthy that a higher than the baseline level of the cerebral hemodynamic parameter APC is observed for hypercapnia with durations of 60 and 120 s, which is probably associated with a compensatory reaction of the blood flow.

To quantify the effect of hypercapnia on hemodynamic indices, we introduced a group-average normalized difference ΔX in every index for each group and each hypercapnia duration as

$$\Delta X = (X_H - X_B)/X_B, \quad (1)$$

where X_H is one of the measurable parameters (CO_2 , ABP, PP, APC, and HR) averaged over hypercapnia duration, and X_B is the same parameter, averaged over the baseline. Table 2 shows the normalized differences in the hemodynamic parameters of rats with different state of the skull at different hypercapnia duration.

Table 2. Normalized difference in hemodynamic indices due to hypercapnia of various duration

Index	CCW			OSD			OCW		
	30 s	60 s	120 s	30 s	60 s	120 s	30 s	60 s	120 s
ΔCO_2 , rel. un.	1.37	1.46	1.52	1.62	1.71	1.70	1.48	1.58	1.56
ΔABP , rel. un.	0.26	0.37	0.05 ^a	-0.27	-0.44	-0.45	-0.34	-0.47	-0.43
ΔPP , rel. un.	0.23	0.24	-0.08 ^a	-0.25	-0.48	-0.49	-0.34	-0.49	-0.48
ΔAPC , rel. un.	0.64	0.77	0.47	0.19	-0.17	-0.28	-0.14	-0.30	-0.37
ΔHR , rel. un.	-0.01	-0.03	-0.09	-0.02	-0.05	-0.11	-0.03	-0.07	-0.18

^a $P > 0.05$.

As seen from Table 2, the changes caused by hypercapnia were statistically significant for most of the indicators. Note that in most cases, hypercapnia resulted in a HR decrease. The only exception was the CCW group at 30-s hypercapnia. At the same time, 30-second hypercapnia led to significant increases in ABP, PP and APC for the CCW group, whereas these parameters were reduced in the OCW group. Bidirectional change in hemodynamic parameters was observed in the OSD group during 30-s hypercapnia: with a decrease in blood pressure, APC significantly increased. However, this increase was not as high as in the CCW group: 0.19 vs 0.64 rel.un.

In the OCW group, an increase in CO_2 exposure resulted in a consistent decrease in both systemic (ABP and PP) and local parameters (APC). Nevertheless, in the OSD group, an increase in APC observed at shorter 30-s hypercapnia (0.19 rel.un., $P < 0.005$) was replaced by its significant decrease with a longer 60-s CO_2 exposure (-0.17 rel.un., $P < 0.005$). The APC decreased to an even greater extent during 120-s hypercapnia: -0.28 rel.un., $P < 0.001$. Note that changes in ABP and PP as a function of the hypercapnia duration were the same in these (OCW and OSD) groups.

In the CCW group, the changes in ABP, PP, and APC due to 30 s of CO_2 exposure were similar to those with hypercapnia lasting 60 seconds. However, completely different character of the changes in the systemic parameters was observed with hypercapnia of 120-s duration: changes in both ABP and PP were insignificant, $P > 0.1$ for both indices (see Table 2). We assume that this was due to the reversal of the direction of changes in both indices in the second half of the longest CO_2 exposure: growth of the systemic parameters during first 60 s is replaced by their diminishing from 60 to 120 s as shown by blue lines in the graphs (A2) and (A3) in Fig. 2. This reverse dynamic of the systemic parameters is accompanied by a fourfold decrease in APC during 120 s of CO_2 exposure compared to 60-s hypercapnia: 0.16 vs 0.78 rel.un.

3.2. The role of systemic hemodynamics

Correlation analysis of hemodynamic parameters revealed that the dynamics of both ABP and PP was associated with the dynamics of APC in all except one group of the studied animals. The correlation coefficients between these parameters for different groups and different hypercapnia duration are shown in Table 3. As one can see, strong positive correlation between systemic and local parameters was observed in most of the groups. The only exception was the OSD group at hypercapnia of 30 s duration in which the correlation coefficient between PP and APC was much lower than in other cases, and no correlation was observed between ABP and APC. Obviously, this is due to the previously described inconsistency in the dynamics of the parameters in this case (see Table 2). It is worth noting that the systemic parameters ABP and PP were strongly

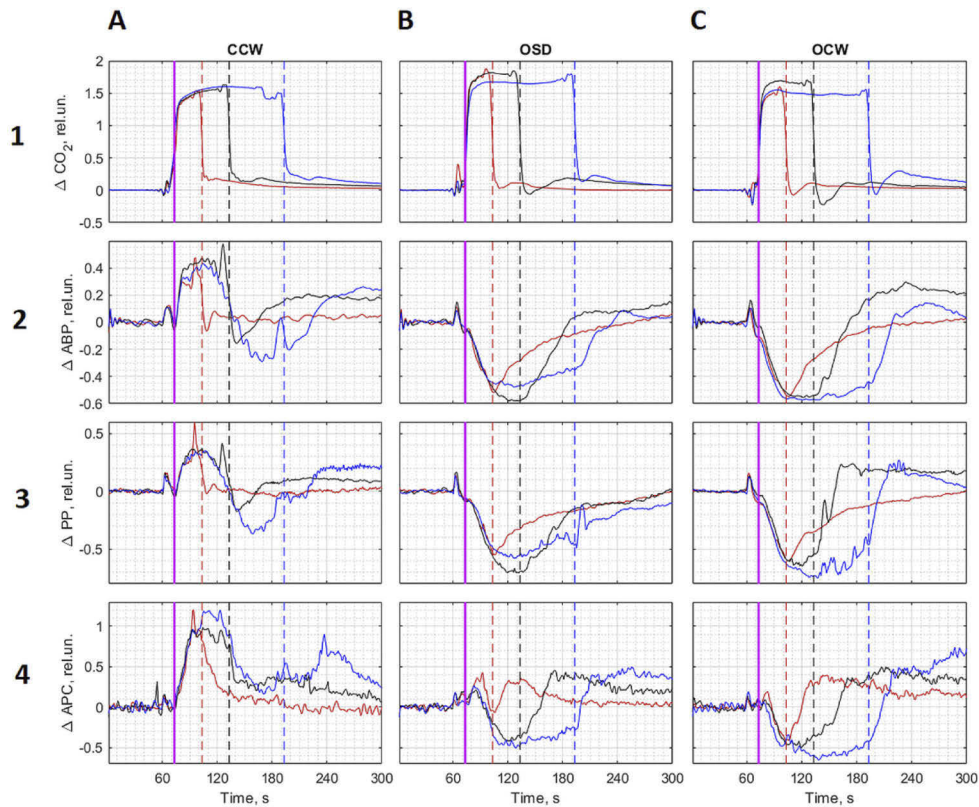


Fig. 2. Reaction of the hemodynamic parameters to hypercapnia of different duration. Columns (A), (B), and (C) shows the graphs for the groups of rats with closed cranial window, open skull but intact dura mater, and open skull with removed dura mater, respectively. Row (1) shows overlaid graphs with averaged relative dynamics of the concentration of end-tidal CO_2 for different duration of hypercapnia. Rows (2), (3), and (4) show overlaid graphs with the responses of the mean systemic blood pressure (ABP), pulse pressure (PP), and the amplitude of the pulsatile component (APC), respectively. The relative changes in the hemodynamic parameters were averaged over each group of rats. Red, black, and blue lines in all graphs show evolutions of the parameters for hypercapnia with duration of 30, 60, and 120 s, respectively. Bold magenta vertical lines indicate the beginning of hypercapnia. Dashed red, black and blue vertical lines indicate hypercapnia lasting 30, 60, and 120 s, respectively. Axis labels and scale grids are identical for every column and every row.

correlated with each other: the correlation coefficient varied between 0.93 and 0.99, $P < 0.0001$ in all cases.

The strong correlation between systemic and local hemodynamic indices in the overwhelming majority of cases indicates the dominant effect of systemic hemodynamics on the state of cortical blood flow, regardless of the local effect of hypercapnia on cerebral vessels. In other words, an increase or decrease in ABP is accompanied by a consistent PP response, which determines a corresponding increase or decrease in blood pulsation in the cerebral vessels assessed by the APC parameter. Notably that changes in systemic hemodynamics caused by the hypercapnia affect APC more significantly than direct effect of CO_2 on cerebral vessels. This circumstance does not allow the use of APC as the only parameter for assessing the cerebrovascular functional reserve, the value of which can be judged either by an increase in cerebral blood flow or by a

Table 3. Correlation coefficients of the group-averaged parameters ABP, PP, and APC at different CO₂ exposure in animals with different state of the skull

Group of rats	Hemodynamics parameters	CO ₂ exposure		
		30 s	60 s	120 s
CCW, <i>n</i> = 8	Correlation of ABP and APC	0.84	0.93	0.84
	Correlation of PP and APC	0.88	0.88	0.65
OSD, <i>n</i> = 13	Correlation of ABP and APC	0.01 ^a	0.70	0.75
	Correlation of PP and APC	0.17	0.75	0.82
OCW, <i>n</i> = 10	Correlation of ABP and APC	0.87	0.93	0.90
	Correlation of PP and APC	0.93	0.96	0.92

^a*P* > 0.05

decrease in regional peripheral resistance. In the next Section, we propose to use multimodal approach for functional reserve assessment.

3.3. Assessment of regional cerebral vascular resistance

Since the response of systemic pressure to hypercapnia varies greatly (up to the opposite sign of dynamics) in different states of the skull, this complicates the assessment of the effect of hypercapnia on cerebral blood flow. Despite a decrease in vascular tone, which creates preconditions for an increase in the pulsatile component, with a decrease in the level of systemic blood pressure, the pulsation of cerebral vessels decreases due to a proportional decrease in perfusion pressure. Most likely, it is oppositely directed influence of local and systemic factors in a number of cases that determines the opposite direction of changes in ABP and APC during a hypercapnia.

Pulse pressure is the main driver of blood pulsations in the vessels. Therefore, in the first approximation, a change in the optically measured parameter APC is proportional to the change in PP. Additionally, changes in APC are inversely proportional to changes in regional peripheral vascular resistance, RPVR. This relationship can be expressed as

$$\Delta APC \propto \Delta PP / \Delta RPVR \text{ or } \Delta RPVR \propto \Delta PP / \Delta APC \quad (2)$$

Since in our experimental setting, systemic PP is highly correlated with the mean ABP, changes in APC are also directly proportional to changes in mean ABP. If we assume that the functional effect of a change in CO₂ concentration on the vascular system is only a change in systemic parameters, then the ratio of the normalized differences in ABP and APC should remain constant during hypercapnia. Nevertheless, it is known that even with a constant systemic pressure, the tone of the cerebral vessels can change, for example, with the dorzolamide injection [27]. A decrease in vascular tone leads to a decrease in regional vascular resistance and, at the same time, to an increase in the amplitude of pulsations, measured by the APC parameter. If such additional changes in cerebral arterial tone occur, the ratio of the normalized differences ABP and APC ($\Delta ABP / \Delta APC$) will reflect them, representing changes in vascular resistance, thus serving as a marker of functional blood flow reserve.

Figure 3 shows evolution of the normalized $\Delta ABP / \Delta APC$ calculated for different groups of animals and different durations of hypercapnia. As one can see, this ratio decreased with an increase of CO₂ in all cases, despite the fact that in different groups the changes in systemic ABP had the opposite sign, which is clearly seen in Fig. 2 (row 2). This fact indicates a decrease in RPVR in response to hypercapnia. Let us introduce the amplitude of RPVR decrease, A_{RPVR} , due to hypercapnia as

$$A_{RPVR} = (\Delta ABP / \Delta APC)_B - (\Delta ABP / \Delta APC)_{min}. \quad (3)$$

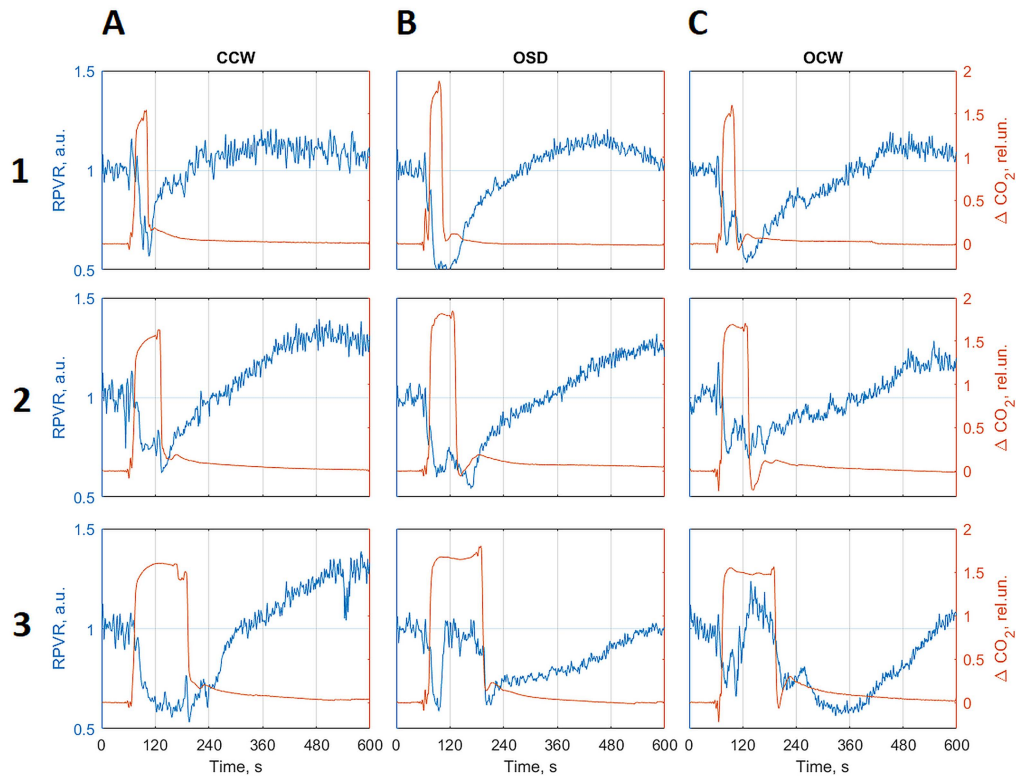


Fig. 3. Dynamics of cerebral vascular resistance in response to hypercapnia. Columns (A), (B), and (C) shows the graphs for the groups of rats with closed cranial window, open skull but intact dura mater, and open skull with removed dura mater, respectively. Rows (1), (2), and (3) show changes in cerebral vascular resistivity to hypercapnia with duration of 30, 60, and 120 s, respectively. Axis labels and scale grids are identical for every column and every row.

Here $(\Delta ABP/\Delta APC)_B$ is the mean ratio of the hemodynamic parameters in the baseline, and $(\Delta ABP/\Delta APC)_{min}$ is the minimal value of the ratio caused by hypercapnia. The amplitude of the RPVR drop is shown in the Table 4. It is worth noting that within each group, A_{RPVR} turns out to be the same for different durations of hypercapnia. After the hypercapnia, the ratio $\Delta ABP/\Delta APC$ is slowly restored in all cases.

Table 4. The amplitude of changes in vascular resistance at different CO₂ exposure in animals with different state of the skull

Group of rats	CO ₂ exposure		
	30 s	60 s	120 s
CCW, $n = 8$	0.41	0.43	0.43
OSD, $n = 13$	0.52	0.53	0.49
OCW, $n = 10$	0.43	0.32	0.34

Since the RPVR dynamics is a measure of hypercapnic vasodilation, this parameter can be used to assess the functional reserve of cortical vessels regardless of the behavior of systemic pressure. Considering the simplicity of the test, the physiological nature of the impact, and contactless character of measurements, the assessment of the functional reserve can be carried

out under the conditions of surgical intervention on the brain. This can be achieved by briefly increasing the CO₂ concentration in the inhaled air by 5% for a patient who is intubated during surgery. Note that such an impact can be repeated several times during the surgery both to clarify the diagnosis and to control the effectiveness of the correction.

4. Discussion

Our experiments have demonstrated that iPPG allows non-contact assessment of changes in intracranial blood flow in response to hypercapnia using the APC parameter, which is a measure of the tone of cerebral vessels. At the same time, transient hypercapnia also leads to changes in systemic hemodynamic parameters such as mean arterial pressure, pulse pressure, and heart rate. Furthermore, it was found that the state of the skull significantly alters the response of both local and systemic hemodynamics: while both types of the parameters are increasing due to hypercapnia in rats with a closed skull, a decrease in these parameters is observed in rats with an open skull. This difference in responses can be explained by competition between different physiological reactions during the hypercapnic test. This is a key point in the interpretation of the test results, since most methods for assessing functional reserve are used with a closed skull as part of preoperative preparation. On the one hand, most neurosurgical operations are performed using craniotomy. On the other hand, a concordant change in systemic blood pressure and amplitude of blood pulsation in the cerebral vessels in response to hypercapnia seriously complicates the interpretation of the results. We assume that the response to hypercapnia includes both the direct vasodilation effect of CO₂ and the compensatory activation of the peripheral and central chemoreflexes [8,31,32]. Note that the direct effect of CO₂ on systemic hemodynamic parameters due to myogenic vasodilation exceeds the reflex effect that is manifested in an immediate decrease in blood pressure in rats with the open skull and in a delayed decrease in rats with the closed skull.

In rats with closed skull, in addition to direct vasodilation and chemoreflexes in response to CO₂, there is also Cushing response [33] that manifests itself by a significant increase in peripheral resistance, which leads to an increase in systemic pressure in response to intracranial hypertension. The origin of the hypertension is explained by the reflex response to hypoperfusion, which occurs due to cerebral edema in a closed skull. In our experiment, cerebral edema is provoked by an increase in cerebral perfusion due to the direct effect of CO₂ on cerebral vessels, which leads to secondary increase in cerebral pressure and triggers the Cushing response. Previously, such a reaction was interpreted as the influence of chemoreflexes in patients with sleep apnea syndrome [34]. However, in rats with an open skull and a removed dura mater, no increase in systemic pressure was observed. Our observations imply revisiting the widespread belief that the chemoreflex is the sole cause of hypertension during sleep apnea. We hypothesize that even in this case, the Cushing's reflex may be the cause of the hypertension.

Obviously, the formation of the PPG waveform is influenced by both systemic blood pressure and regional vascular resistance, see Eq. (2). It is worth noting that it is the dynamics of RPVR that is a measure of the functional reserve. Considering the role of perfusion and mean ABP in maintaining local blood flow, the exclusion of the systemic hemodynamic factor is required to assess the effect of hypercapnia on the tone of cerebral vessels. This was done by calculating the ratio of PP change and APC change (Eq. (2)), which represents the desired dynamics of regional peripheral resistance. Therefore, the ratio of the dynamics of systemic blood pressure and local blood perfusion measured by APC allows assessing the functional reserve of cerebral vessels regardless of the behavior of systemic hemodynamics in response to CO₂ exposure. RPVR is an indicator that is necessary for every surgeon involved in brain revascularization, not only to clarify the diagnosis but also to assess the effectiveness of the surgical intervention.

The method of intraoperative assessment of the functional reserve of cerebral vessels was developed based on the results of an experimental study of animals. It is clear that more in-depth

research in humans is needed for the successful implementation of this method in the clinical environment.

5. Conclusion

The reaction of systemic and local (cerebral) hemodynamics in response to hypercapnia under conditions of a closed and open skull is significantly different, which is explained by the additional vasopressor reflex of Cushing in the case of intact cranial bone. Regardless of the state of the skull, the vasodilatation effect of hypercapnia can be assessed by means of the ratio of PP to APC changes, the latter being measured using contactless iPPG. The method of non-contact assessment of the functional reserve of cerebral vessels using iPPG can be used during neurosurgical revascularization for detailed diagnosis and evaluation of the results of surgical treatment.

Funding. Russian Science Foundation (21-15-00265); Ministry of Education and Science of the Russian Federation (075-15-2020-800).

Acknowledgments. This research was financially supported by the Russian Science Foundation (Grant No. 21-15-00265) in the part of development of high-speed iPPG system and the computer software for experimental data processing and by the Ministry of Education and Science of the Russian Federation (Grant No. 075-15-2020-800) in the part of carrying out the experimental study and theoretical analysis of the obtained results.

Disclosures. The authors declare that there are no conflicts of interest related to this article.

Data availability. Data underlying the results presented in this paper are not publicly available at this time but may be obtained from the authors upon reasonable request.

References

1. O. Puig, O. M. Henriksen, M. B. Vestergaard, A. E. Hansen, F. L. Andersen, C. N. Ladefoged, E. Rostrup, H. B. W. Larsson, U. Lindberg, and I. Law, "Comparison of simultaneous arterial spin labeling MRI and ^{15}O -H $_2\text{O}$ PET measurements of regional cerebral blood flow in rest and altered perfusion states," *J. Cereb. Blood Flow Metab.* **40**(8), 1621–1633 (2020).
2. P. Liu, J. B. De Vis, and H. Lu, "Cerebrovascular reactivity (CVR) MRI with CO $_2$ challenge: a technical review," *NeuroImage* **187**, 104–115 (2019).
3. K. Kohshi, Y. Kinoshita, and K. Fukata, "Brain pH responses to acetazolamide and hypercapnia in cats," *Neurol. Med. Chir. (Tokyo)* **37**(4), 313–319 (1997).
4. G. Settakis, C. Molnar, L. Kerenyi, J. Kollar, D. Legemate, L. Csiba, and B. Fulesdi, "Acetazolamide as a vasodilatory stimulus in cerebrovascular diseases and in conditions affecting the cerebral vasculature," *Eur. J. Neurol.* **10**(6), 609–620 (2003).
5. M. Reivich, "Arterial PC $_2$ and cerebral hemodynamics," *Am. J. Physiol.* **206**(1), 25–35 (1964).
6. R. T. R. Huckstepp and N. Dale, "CO $_2$ -dependent opening of an inwardly rectifying K $^+$ channel," *Pflugers Arch.* **461**(3), 337–344 (2011).
7. R. L. Hoiland, J. A. Fisher, and P. N. Ainslie, "Regulation of the cerebral circulation by arterial carbon dioxide," *Compr. Physiol.* **9**, 1101–1154 (2011).
8. D. A. Keir, J. Duffin, P. J. Millar, and J. S. Floras, "Simultaneous assessment of central and peripheral chemoreflex regulation of muscle sympathetic nerve activity and ventilation in healthy young men," *J. Physiol.* **597**(13), 3281–3296 (2019).
9. T. Kara, K. Narkiewicz, and V. K. Somers, "Chemoreflexes - physiology and clinical implications," *Acta Physiol. Scand.* **177**(3), 377–384 (2003).
10. O. A. Lyubashina, O. V. Mamontov, M. A. Volynsky, V. V. Zaytsev, and A. A. Kamshilin, "Contactless assessment of cerebral autoregulation by photoplethysmographic imaging at green illumination," *Front. Neurosci.* **13**, 1235 (2019).
11. J. Petersson and R. W. Glenny, "Gas exchange and ventilation-perfusion relationships in the lung," *Eur. Respir. J.* **44**(4), 1023–1041 (2014).
12. A. L. Urback, B. J. MacIntosh, and B. I. Goldstein, "Cerebrovascular reactivity measured by functional magnetic resonance imaging during breath-hold challenge: a systematic review," *Neurosci. Biobehav. Rev.* **79**, 27–47 (2017).
13. E. Sleight, M. S. Stringer, J. Marshall, J. M. Wardlaw, and M. J. Thrippleton, "Cerebrovascular reactivity measurement using magnetic resonance imaging: a systematic review," *Front. Physiol.* **12**, 643468 (2021).
14. M. N. McDonnell, N. M. Berry, M. A. Cutting, H. A. Keage, J. D. Buckley, and P. R. C. Howe, "Transcranial Doppler ultrasound to assess cerebrovascular reactivity: reliability, reproducibility and effect of posture," *PeerJ* **1**, e65 (2013).
15. H. J. Steiger, R. Aaslid, and R. Stooss, "Dynamic computed tomographic imaging of regional cerebral blood flow and blood volume. A clinical pilot study," *Stroke* **24**(4), 591–597 (1993).
16. T. Kunieda, K. Miyake, K. Sakamoto, Y. Iwasaki, S. Iida, S. Morise, K. Fujita, M. Nakamura, S. Kaneko, and H. Kusaka, "Leptomeningeal collaterals strongly correlate with reduced cerebrovascular reactivity measured by

- acetazolamide-challenged single-photon emission computed tomography using a stereotactic extraction estimation analysis in patients with unilateral internal,” *Intern. Med.* **56**(21), 2857–2863 (2017).
17. T. H. Wong, Q. A. Shagera, H. G. Ryoo, S. Ha, and D. S. Lee, “Basal and acetazolamide brain perfusion SPECT in internal carotid artery stenosis,” *Nucl. Med. Mol. Imagin.* **54**(1), 9–27 (2020).
 18. D. Milej, M. Shahid, A. Abdalmalak, A. Rajaram, M. Diop, and K. St. Lawrence, “Characterizing dynamic cerebral vascular reactivity using a hybrid system combining time-resolved near-infrared and diffuse correlation spectroscopy,” *Biomed. Opt. Express* **11**(8), 4571–4585 (2020).
 19. T. Pham, G. Blaney, A. Sassaroli, C. Fernandez, and S. Fantini, “Sensitivity of frequency-domain optical measurements to brain hemodynamics: simulations and human study of cerebral blood flow during hypercapnia,” *Biomed. Opt. Express* **12**(2), 766–789 (2021).
 20. B. A. Sutherland, T. Rabie, and A. M. Buchan, “Laser Doppler flowmetry to measure changes in cerebral blood flow,” in *Cerebral Angiogenesis*, R. Milner, ed., Methods in Molecular Biology (Humana Press, 2014), 1135(20), pp. 237–248.
 21. J. Tonnesen, A. Pryds, E. H. Larsen, O. B. Paulson, J. Hauerberg, and G. M. Knudsen, “Laser Doppler flowmetry is valid for measurement of cerebral blood flow autoregulation lower limit in rats,” *Exp. Physiol.* **90**(3), 349–355 (2005).
 22. F. A. Zeiler, J. Donnelly, D. Cardim, D. K. Menon, P. Smielewski, and M. Czosnyka, “ICP versus laser Doppler cerebrovascular reactivity indices to assess brain autoregulatory capacity,” *Neurocrit. Care* **28**(2), 194–202 (2018).
 23. B. R. Rosenblum, R. F. Bonner, and E. H. Oldfield, “Intraoperative measurement of cortical blood flow adjacent to cerebral AVM using laser Doppler velocimetry,” *J. Neurosurg.* **66**(3), 396–399 (1987).
 24. P. Castro, E. Azevedo, and F. Sorond, “Cerebral autoregulation in stroke,” *Curr. Atheroscler. Rep.* **20**(8), 37 (2018).
 25. J. Fierstra, J.-K. Burkhardt, C. H. B. van Niftrik, M. Piccirelli, A. Pangalu, R. Kocian, M. C. Neidert, A. Valavanis, L. Regli, and O. Bozinov, “Blood oxygen-level dependent functional assessment of cerebrovascular reactivity: Feasibility for intraoperative 3 Tesla MRI,” *Magn. Reson. Med.* **77**(2), 806–813 (2017).
 26. G. Muscas, C. H. B. van Niftrik, J. Fierstra, M. Piccirelli, M. Sebok, J.-K. Burkhardt, A. Valavanis, A. Pangalu, L. Regli, and O. Bozinov, “Feasibility and safety of intraoperative BOLD functional MRI cerebrovascular reactivity to evaluate extracranial-to-intracranial bypass efficacy,” *Neurosurg. Focus* **46**(2), E7 (2019).
 27. O. V. Mamontov, A. Y. Sokolov, M. A. Volynsky, A. V. Osipchuk, V. V. Zaytsev, R. V. Romashko, and A. A. Kamshilin, “Animal model of assessing cerebrovascular functional reserve by imaging photoplethysmography,” *Sci. Rep.* **10**(1), 19008 (2020).
 28. A. A. Kamshilin, T. V. Krasnikova, M. A. Volynsky, S. V. Miridonov, and O. V. Mamontov, “Alterations of blood pulsations parameters in carotid basin due to body position change,” *Sci. Rep.* **8**(1), 13663 (2018).
 29. I. S. Sidorov, M. A. Volynsky, and A. A. Kamshilin, “Influence of polarization filtration on the information readout from pulsating blood vessels,” *Biomed. Opt. Express* **7**(7), 2469–2474 (2016).
 30. A. Y. Sokolov, M. A. Volynsky, V. V. Zaytsev, A. V. Osipchuk, and A. A. Kamshilin, “Advantages of imaging photoplethysmography for migraine modeling: new optical markers of trigemino-vascular activation in rats,” *J. Headache Pain* **22**(1), 18 (2021).
 31. S. Yoon, M. Zuccarello, and R. M. Rapoport, “pCO₂ and pH regulation of cerebral blood flow,” *Front. Physiol.* **3**, 365 (2012).
 32. P. N. Ainslie and J. Duffin, “Integration of cerebrovascular CO₂ reactivity and chemoreflex control of breathing: mechanisms of regulation, measurement, and interpretation,” *Am. J. Physiol. Regul. Integr. Comp. Physiol.* **296**(5), R1473–R1495 (2009).
 33. W. H. Wang, B. T. Ang, and E. Wang, “The Cushing response: a case for a review of its role as a physiological reflex,” *J. Clin. Neurosci.* **15**(3), 223–228 (2008).
 34. N. R. Prabhakar, “Carotid body chemoreflex: a driver of autonomic abnormalities in sleep apnoea,” *Exp. Physiol.* **101**(8), 975–985 (2016).